Cooperative formation control of underactuated marine vehicles for target surveillance under sensing and communication constraints

Dimitra Panagou and Kostas J. Kyriakopoulos

Abstract— **This paper presents a Leader-Follower formation control strategy for underactuated marine vehicles which move under sensing and communication constraints in the presence of bounded persistent environmental disturbances. We assume that the vehicles do not communicate for exchanging information regarding on their states (pose and velocities), and that their sensing capabilities are restricted, due to limited range and angle-of-view. Sensing constraints are thus realized as a set of inequality state constraints which should never be violated (viability constraints). The viability constraints define a closed subset K of the configuration space (viability set K). The control objective is thus reduced into to coordinating the motion of the vehicles in a Leader-Follower formation, while system trajectories starting in K always remain viable in K. The proposed control design employs dipolar vector fields and a viability-based switching control scheme, which guarantees that system viability is always maintained. The efficacy of the proposed algorithm, as well as its relevance with surveillance of (stationary) targets are demonstrated through simulations.**

I. Introduction

Multi-vehicle systems and cooperative control objectives have recently seen an increased interest within the fields of marine robotics and oceanic engineering. Applications such as environmental monitoring, surveillance and scientific explorations, search and rescue missions, harbor patrol, situation awareness, motivate the development of distributed systems of relatively lower cost and power, to carry out a common task in a collaborative manner. Coordinating the motion of marine vehicles in *formations* is a characteristic paradigm of achieving collective behaviors and complicated tasks, compared to employing a single vehicle. Multi-vehicle formations can be used, among others, for seabed mapping, structure inspection (pipelines, oil drilling platforms), offshore and inshore surveillance; therefore, the coordination and formation control for multiple *underactuated* marine vehicles has been and still remains an active topic of research.

Choosing a pertinent formation strategy is primarily depended on the nature of the application at hand, as well as on the information flow among the vehicles. For the case of marine applications in particular, note that underwater communications and sensing rely mostly on acoustic systems, which suffer from limited range and communication bandwidth; thus, such constraints impose challenges and in principle can not be ignored during the control design.

This work has been supported by Qatar National Research Fund under NPRP Grant 4-536-2-199. Dimitra Panagou is with the Coordinated Science Laboratory, College of Engineering, University of Illinois at Urbana-Champaign, Urbana, IL, USA dpanagou@illinois.edu

Kostas Kyriakopoulos is with the Control Systems Lab, School of Mechanical Engineering, National Technical University of Athens, Greece kkyria@mail.ntua.gr

Popular ways to address the formation control for multiple marine vehicles have been the coordinated path following of pre-described spatial paths while keeping desired inter-vehicle formation patterns [1]–[4] and tracking of reference trajectories [5], [6]. Behavioral-based approaches have been presented in [7], [8], while geometric methods that rely on the virtual structure paradigm have appeared in [9], [10].

Leader - Follower $(\mathrm{L}-\mathrm{F})$ formation strategies have also been widely studied, mainly due to their simplicity in control design and scalability in implementation. In a $\mathrm{L}-\mathrm{F}$ formation, L tracks a predefined path while F maintains a desired geometric configuration with respect to (w.r.t.) L. Consequently, the local control design is strongly depended on the information that F can access regarding on the states of L. For instance, the formation control designs in [11], [12] require an intermittent or periodic broadcast of the position and velocities of L to F. In [13] F can obtain any information from L, while the decentralized control design in [14] assumes that each vehicle obtains information from one or two neighboring vehicles. In [15], F acquires the position of L to track a reference trajectory in accordance with a predefined distance, without any information on the leader's velocity and dynamics. In [16] all vehicles are first forced to follow predefined paths, with L moving with the desired formation speed, and then the velocities of F are coordinated with a single communication broadcast from L. In general, the communication variable broadcast in a $\mathrm{L}-\mathrm{F}$ strategy is required to be kept to a minimum, due to the constraints of the acoustic communication bandwidth.

Motivated in part by this remark, in this paper we consider a surveillance scenario, in which two marine vehicles have to move on the horizontal plane in $\mathrm{L}-\mathrm{F}$ formation with no explicit communication and information exchange between them. Each vehicle is assumed to carry an onboard sensor with limited range and angle-of-view; for example, a forward-looking sonar on an underwater vehicle, or a camera on a surface vessel. These limitations define the effective sensing area of each vehicle as a circular sector of radius L and angle $2a$ (Fig. 1). Thus, each vehicle can track and acquire reliable measurements on the pose of objects lying within its sensing area. L is assigned with the task to move in the proximity of and always keep a (stationary) target T visible in its sensing area, while F is required to maintain a fixed distance and orientation w.r.t. to L.[1] Consequently, due to sensing and communication limitations, it immediately

[1]In this scenario we rather treat F as a back-up vehicle, and do not have it assigned with the task of *directly* surveilling the target T. Nevertheless, as illustrated in Section IV, F may also gradually gain visibility with T.

follows that coordinating the motion of the vehicles in a $\mathrm{L-F}$ fashion for target surveillance can be effective if and only if L maintains visibility with T, and F maintains visibility with L.

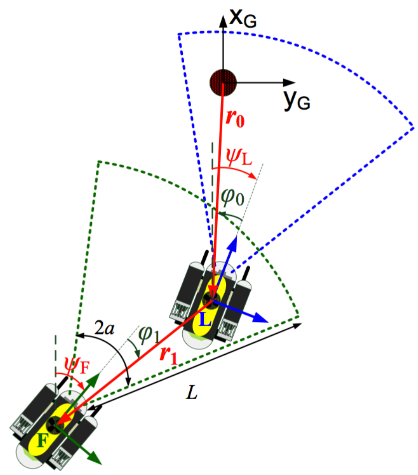

Fig. 1. Each vehicle can sense and be localized w.r.t. objects within its sensing area.

To this end, we build upon earlier work of ours [17], [18] and adopt notions from viability theory [19] as follows: the requirements imposed by the limited sensing are realized as a set of hard inequality constraints w.r.t. the configuration variables, called *viability constraints*. The viability constraints constitute a subset K of the configuration space, called the *viability set* K of the system. System trajectories that always belong into K are called *viable*, whereas those which either start out of K, or escape K for some $t > 0$, immediately violate the viability constraints and thus are not acceptable.

Then, the control objective is translated into designing state feedback control laws so that the vehicles move in $\mathrm{L-F}$ formation, while the resulting trajectories remain viable in K. The control design is characterized as cooperative, in the sense that the vehicles are not thought of as a pair of one pursuer, one evader, with the latter trying to escape the sensing area of the former, but on the contrary are controlled so that each one always keeps its target visible in its sensing area. The proposed control algorithms guarantee that the system trajectories are (i) viable in K, i.e. that each vehicle always maintains visibility w.r.t. its target while moving in $\mathrm{L-F}$ fashion, as well as (ii) collision-free.

Compared to other relevant solutions on $\mathrm{L-F}$ formation control for marine vehicles, our algorithms do not require any communication or information exchange between the vehicles regarding on their states; only the upper bounds of the leader's velocities are assumed to be a priori known to the follower. In this way, the task is executed in a distributed manner, with each vehicle taking care of converging to a desired distance, while maintaining visibility with, its target. Furthermore, our path planning and control algorithms guarantee that inter-vehicle collisions are always avoided, something which is often taken for granted in similar $\mathrm{L-F}$ approaches. Compared to our previous work in [18], here we extend our methodology, originally presented for agents with unicycle kinematics, to underactuated marine vehicles, and propose an alternative way of controlling L for maintaining visibility with T. Finally, compared to [17], in this paper we consider a multi-vehicle scenario and furthermore the effect of non-vanishing, bounded external perturbations.

The paper is organized as follows: Section II provides the modeling of the system and of the sensing constraints. Section III includes the proposed control design for the $\mathrm{L-F}$ formation, while its efficacy is demonstrated in Section IV. Our conclusions and plans for future extensions are summarized in Section V.

II. Mathematical Modeling

We consider the horizontal motion of (identical, for simplicity) marine vehicles which have two back thrusters for moving along the surge and the yaw degree-of-freedom (d.o.f.), but no side (lateral) thruster for moving along the sway d.o.f.. Following [20], the kinematics and dynamics for the i vehicle are:

$$\dot{x}_i = u_i \cos\psi_i - v_i \sin\psi_i, \tag{1a}$$
$$\dot{y}_i = u_i \sin\psi_i + v_i \cos\psi_i, \tag{1b}$$
$$\dot{\psi}_i = r_i, \tag{1c}$$
$$m_u \dot{u}_i = m_v v_i r_i + X_u u_i + X_{u|u|} |u_i| u_i + \tau_{ui} + w_u, \tag{1d}$$
$$m_v \dot{v}_i = -m_u u_i r_i + Y_v v_i + Y_{v|v|} |v_i| v_i + w_v, \tag{1e}$$
$$m_r \dot{r}_i = m_{uv} u_i v_i + N_r r_i + N_{r|r|} |r_i| r_i + \tau_{ri} + w_r, \tag{1f}$$

where $i \in \{\mathrm{L}, \mathrm{F}\}$, $\boldsymbol{\eta}_i = \begin{bmatrix}\boldsymbol{r}_i^\top & \psi_i\end{bmatrix}^\top = \begin{bmatrix}x_i & y_i & \psi_i\end{bmatrix}^\top$ is the pose vector w.r.t. a global frame $\mathcal{G}$, $\boldsymbol{r}_i = \begin{bmatrix}x_i & y_i\end{bmatrix}^\top$ is the position vector w.r.t. $\mathcal{G}$, $\boldsymbol{\nu}_i = \begin{bmatrix}u_i & v_i & r_i\end{bmatrix}^\top$ is the vector of linear and angular velocities w.r.t. the body-fixed frame $\mathcal{B}_i$, m_u, m_v, m_r are the terms of the inertia matrix including the added mass effect, $m_{uv} = m_u - m_v$, X_u, Y_v, N_r are linear drag terms, $X_{u|u|}$, $Y_{v|v|}$, $N_{r|r|}$ are nonlinear drag terms, $\boldsymbol{\tau}_i = \begin{bmatrix}\tau_{ui} & 0 & \tau_{ri}\end{bmatrix}^\top$ is the vector of control inputs, and $\boldsymbol{w} = \begin{bmatrix}w_u & w_v & w_r\end{bmatrix}^\top$ is the vector of bounded external disturbances, such that $|w_u| \leq w_{ub}$, $|w_v| \leq w_{vb}$, $|w_r| \leq w_{rb}$.

Each vehicle i is localized w.r.t. objects which lie in its sensing area, i.e. the position vectors $\boldsymbol{r}_j = \begin{bmatrix}x_j & y_j\end{bmatrix}^\top$, $j \in \{0, 1\}$ and the bearing angles $\phi_j \in [-a, a]$ are measured (Fig. 1). Consequently, reliable pose feedback w.r.t. a target of interest is available to each vehicle i if and only if $|\phi_j| \leq a$ and $\|\boldsymbol{r}_j\| \leq L$, where $L > 0$ is the maximum effective range and $2a > 0$ is the effective angle-of-view. These constraints define the closed subsets K_j of the configuration space, given as $K_j = \{\boldsymbol{\eta}_j \mid h_{jk}(\boldsymbol{\eta}_j) \leq 0,\ j \in \{0, 1\},\ \ k \in \{1, 2\}\}$, where $h_{j1} = |\phi_j| - a$ and $h_{j2} = \|\boldsymbol{r}_j\| - L$. Thus, for the sensing system to be effective, the trajectories $\boldsymbol{\eta}_j(t)$ should always evolve in the set $K = \bigcup_j K_j$, called the *viability set*.

To describe the motion of L w.r.t. target T, the global frame $\mathcal{G}$ is set on T; then the equations of motion for L are given by (1), with $\boldsymbol{\eta}_{\mathrm{L}} \triangleq \boldsymbol{\eta}_0$. To describe the motion of F w.r.t. the leader frame $\mathcal{B}_{\mathrm{L}}$, take the position vector $\boldsymbol{r}_1 = \begin{bmatrix}x_1 & y_1\end{bmatrix}^\top$ of F w.r.t. $\mathcal{B}_{\mathrm{L}}$, defined as $\boldsymbol{r}_1 = \mathbf{R}(-\psi_{\mathrm{L}})\,(\boldsymbol{r}_{\mathrm{F}} - \boldsymbol{r}_{\mathrm{L}})$, and consider its time derivative as $\dot{\boldsymbol{r}}_1 =$

$\dot{\mathbf{R}}(-\psi_\text{L})\,(\boldsymbol{r}_\text{F}-\boldsymbol{r}_\text{L})+\mathbf{R}(-\psi_\text{L})\,(\dot{\boldsymbol{r}}_\text{F}-\dot{\boldsymbol{r}}_\text{L})$, where $\mathbf{R}(-\psi_\text{L}) = \left[\begin{smallmatrix}\cos(-\psi_\text{L}) & -\sin(-\psi_\text{L})\\ \sin(-\psi_\text{L}) & \cos(-\psi_\text{L})\end{smallmatrix}\right] = \left[\begin{smallmatrix}\cos\psi_\text{L} & \sin\psi_\text{L}\\ -\sin\psi_\text{L} & \cos\psi_\text{L}\end{smallmatrix}\right]$ is the rotation matrix of the frame $\mathcal{B}_\text{L}$ w.r.t. frame $\mathcal{G}$, and $\dot{\mathbf{R}}(-\psi_\text{L}) = \left[\begin{smallmatrix}0 & r_\text{L}\\ -r_\text{L} & 0\end{smallmatrix}\right]\mathbf{R}(-\psi_\text{L})$. After some algebra one eventually gets:

$$\begin{bmatrix}\dot{x}_1\\ \dot{y}_1\\ \dot{\beta}\end{bmatrix} = \begin{bmatrix}c\beta & -s\beta & 0\\ s\beta & c\beta & 0\\ 0 & 0 & 1\end{bmatrix}\begin{bmatrix}u_\text{F}\\ v_\text{F}\\ r_\text{F}\end{bmatrix} + \begin{bmatrix}-1 & 0 & y_1\\ 0 & -1 & -x_1\\ 0 & 0 & -1\end{bmatrix}\begin{bmatrix}u_\text{L}\\ v_\text{L}\\ r_\text{L}\end{bmatrix},$$

where the vector $\boldsymbol{\eta}_1 = [x_1 \;\; y_1 \;\; \beta]^\top$ comprises the position $\boldsymbol{r}_1 = [x_1 \;\; y_1]^\top$ and orientation β of F w.r.t. frame $\mathcal{B}_\text{L}$, $c\beta$ and $s\beta$ stand for $\cos\beta$ and $\sin\beta$, respectively, while the evolution of the velocities u_i, v_i, r_i is governed by the dynamic equations in (1). As expected, the motion of L can be seen as a perturbation to the motion of F.

III. Control Design

Following common practice for this class of vehicles, we first consider the subsystem Σ_{1i} of kinematic equations (1a)-(1c) augmented with the sway dynamics (1e) for each vehicle i, and design *virtual* control laws $\gamma_{i1}(\cdot)$, $\gamma_{i2}(\cdot)$ for the linear and the angular velocity, respectively. Then, a control law for the actual control inputs τ_{ui}, τ_{ri} is designed via backstepping and feedback linearization, so that the actual velocities u_i, r_i track the virtual velocities $\gamma_{i1}(\cdot)$, $\gamma_{i2}(\cdot)$.

A. Control design for the Leader

1) Necessary and sufficient conditions for maintaining visibility: In order to ensure that the trajectories $\boldsymbol{\eta}_0(t)$ remain into the set K_0 for all $t \geq 0$, one has to ensure that, at all points of the boundary ∂K_0, the system vector field points into the interior of K_0, so that the resulting solution is brought back into K_0 [19]. Thus, given that the constraints $h_{0k}(\cdot) : \mathbb{R}^3 \to \mathbb{R}$ are continuously differentiable functions, one has thus to control the motion of L while ensuring that at all points $\bar{\boldsymbol{\eta}}_0$ on the boundary ∂K_0 the following conditions hold: $\dot{h}_{0k}(\bar{\boldsymbol{\eta}}_0) = \nabla h_{0k}\,\dot{\boldsymbol{\eta}}_0 < 0$, for each k.

2) Path following: Building upon previous work of ours we design a controller for the motion of L based on the concept of reference *dipolar* vector fields.

A dipolar vector field $\mathbf{F} : \mathbb{R}^2 \to \mathbb{R}^2$ is described by:

$$\mathbf{F}(\boldsymbol{r}) = \lambda(\boldsymbol{p}^\top\boldsymbol{r})\boldsymbol{r} - \boldsymbol{p}(\boldsymbol{r}^\top\boldsymbol{r}), \tag{2}$$

where $\lambda \geq 2$, $\boldsymbol{p} \in \mathbb{R}^2$ and $\boldsymbol{r} = [x \;\; y]^\top$ is the position vector w.r.t. $\mathcal{G}$. The main characteristic is that all its integral lines converge to $(0,0)$, tangent to the direction $\varphi_p = \operatorname{atan2}(p_y, p_x)$ of the vector $\boldsymbol{p} = [p_x \;\; p_y]^\top$. Then, picking a vector $\boldsymbol{p}$ such that $\varphi_p \triangleq \psi_d$ reduces the orientation control design into forcing the vehicle to align with the integral curves of $\mathbf{F}(\cdot)$. We therefore define the following reference dipolar vector field $\mathbf{F}_\text{L}(\cdot)$ for L, with analytic form taken out of (2), where the vector $\boldsymbol{r}$ is substituted by the position error vector $\boldsymbol{r}_e = [x_e \;\; y_e]^\top$, where $\boldsymbol{r}_e \triangleq \boldsymbol{r}_0 - \boldsymbol{r}_{0d}$, $\boldsymbol{r}_{0d} = [x_{0d} \;\; y_{0d}]^\top$ is the desired position for L, $\boldsymbol{p} \triangleq \boldsymbol{p}_\text{L} = [p_x^\text{L} \;\; p_y^\text{L}]^\top$ and $\lambda = 2$:

$$\text{F}_x^\text{L} = p_x^\text{L}\,{x_e}^2 - p_x^\text{L}\,{y_e}^2 + 2p_y^\text{L}\,x_e y_e, \tag{3a}$$

$$\text{F}_y^\text{L} = p_y^\text{L}\,{y_e}^2 - p_y^\text{L}\,{x_e}^2 + 2p_x^\text{L}\,x_e y_e. \tag{3b}$$

Theorem 1: The position trajectories $\boldsymbol{r}_0(t)$ of L converge into a ball $B(\boldsymbol{r}_{0d}, \varepsilon_\text{L})$ around the desired position $\boldsymbol{r}_{0d}$ under the (virtual) control law

$$u_\text{L} = -k_1\operatorname{sgn}\left(\boldsymbol{p}_\text{L}^\top\boldsymbol{r}_e\right)\tanh(\|\boldsymbol{r}_e\|), \tag{4a}$$

$$r_\text{L} = -k_2(\psi_\text{L} - \varphi), \tag{4b}$$

where $k_1,\; k_2 > 0$, $\varphi = \operatorname{atan2}(\text{F}_y^\text{L}, \text{F}_x^\text{L})$ is the orientation of the vector field (3) at (x_L, y_L) w.r.t. $\mathcal{G}$, and $\varepsilon_\text{L} > 0$ can be made arbitrarily small.

Proof: In order to study the convergence of the position trajectories $\boldsymbol{r}_0(t)$ into a ball around the desired position we think of the system $\Sigma_{\text{L}\,1}$ as decomposed into two subsystems with different time scales, where the states $\boldsymbol{z} \triangleq [\psi_\text{L} \;\; v_\text{L}]^\top$ constitute the boundary-layer (fast) system, and the states $\boldsymbol{x} \triangleq [x_\text{L} \;\; y_\text{L}]^\top$ constitute the reduced (slow) system. Then, the closed-loop system $\Sigma_{\text{L}\,1}$ under the control law (4b) can be written as a singular perturbation model by considering the (small) parameter $\epsilon \triangleq \frac{1}{k_2}$, for k_2 sufficiently large, as:

$$\begin{aligned}
\dot{x}_\text{L} &= u_\text{L}\cos\psi_\text{L} - v_\text{L}\sin\psi_\text{L}\\
\dot{y}_\text{L} &= u_\text{L}\sin\psi_\text{L} + v_\text{L}\cos\psi_\text{L}\\
\epsilon\dot{\psi}_\text{L} &= -(\psi_\text{L} - \varphi)\\
\epsilon\dot{v}_\text{L} &= \frac{m_u}{m_v}u_\text{L}(\psi_\text{L} - \varphi) + \epsilon\frac{Y_v}{m_v}v_\text{L} + \epsilon\frac{Y_{v|v|}}{m_v}\,|v_\text{L}|\,v_\text{L} + \epsilon\frac{w_v}{m_v}.
\end{aligned}$$

The boundary-layer system has one isolated root: $\psi_\text{L} = \varphi$, given for $\epsilon = 0$. Let us take the error $\eta = \psi_\text{L} - \varphi$; then one can easily verify that $\epsilon\frac{d\eta}{dt} = \epsilon\dot{\psi}_\text{L} - \epsilon\dot{\varphi} = -(\psi_\text{L} - \varphi) - \epsilon\dot{\varphi} \Rightarrow \frac{d\eta}{d\tau} \triangleq -\eta$, where $\epsilon\frac{d\eta}{dt} = \frac{d\eta}{d\tau}$ [21]. This implies that the vehicle orientation ψ_L converges exponentially and at a very fast time scale to the orientation φ of the reference vector field (3).

Let us now consider the candidate Lyapunov function $V = \frac{1}{2}({x_e}^2 + {y_e}^2)$ for the reduced (slow) subsystem, and take the derivative of V along the system trajectories, evaluated at the stable equilibrium $\eta = 0$ of the boundary-layer subsystem, that is for $\psi_\text{L} = \varphi$:

$$\dot{V} = \boldsymbol{r}_e^\top\left[\begin{smallmatrix}u_\text{L}\cos\varphi - v_\text{L}\sin\varphi\\ u_\text{L}\sin\varphi + v_\text{L}\cos\varphi\end{smallmatrix}\right] = \boldsymbol{r}_e^\top\left[\begin{smallmatrix}\cos\varphi\\ \sin\varphi\end{smallmatrix}\right]u_\text{L} + \boldsymbol{r}_e^\top\left[\begin{smallmatrix}-\sin\varphi\\ \cos\varphi\end{smallmatrix}\right]v_\text{L}.$$

As expected, the evolution of $\dot{V}$ depends on the unactuated dynamics via the sway velocity v_L. Since v_L comes from the control input $\zeta = u_\text{L}\,r_\text{L}$, one can resort to an input-to-state stability (ISS) argument to study its evolution, as follows: Consider the candidate ISS-Lyapunov function $V_v = \frac{1}{2}{v_\text{L}}^2$ and take its time derivative

$$\dot{V}_v \leq -\frac{m_u}{m_v}v_\text{L}\zeta - \left(\frac{|Y_v|}{m_v}{v_\text{L}}^2 + \frac{|Y_{v|v|}|}{m_v}\,|v_\text{L}|\,{v_\text{L}}^2 - \frac{|w_v|}{m_v}|v_\text{L}|\right),$$

where $Y_v, Y_{v|v|} < 0$ and $w(v_\text{L}) = \frac{|Y_v|}{m_v}{v_\text{L}}^2 + \frac{|Y_{v|v|}|}{m_v}\,|v_\text{L}|\,{v_\text{L}}^2 - \frac{|w_v|}{m_v}|v_\text{L}|$ is positive definite. Take $\theta \in (0,1)$, then: $\dot{V}_v \leq -(1-\theta)w(v_\text{L})$, $\forall v_\text{L} : -\frac{m_u}{m_v}v_\text{L}\zeta - \theta w(v_\text{L}) \leq 0$. If the control input $\zeta = u_\text{L}\;r_\text{L}$ is bounded, $|\zeta| \leq \zeta_b$, then one has $\dot{V}_v \leq -(1-\theta)w(v_\text{L})$, $\forall |v_\text{L}| : |Y_v||v_\text{L}| + |Y_{v|v|}||v_\text{L}|^2 - |w_v| > \frac{m_u}{\theta}\zeta_b$. Then, the subsystem (1e) is ISS w.r.t. ζ [21, Thm 4.19], which essentially expresses that for any bounded input $\zeta = u_\text{L}\;r_\text{L}$, the linear velocity $v_\text{L}(t)$ will be ultimately bounded by a class $\mathcal{K}$ function of $\sup_{t>0}|\zeta(t)|$. If furthermore $\zeta(t) = u_{\mathrm{L}}(t)\, r_{\mathrm{L}}(t)$ converges to zero as $t \to \infty$, then $v_{\mathrm{L}}(t)$ converges to zero as well [21].

At this point, note that the control input $r_{\mathrm{L}} \triangleq -k_2\eta$ (4b) is bounded and converges to zero at a very fast time scale, since the orientation error $\eta = 0$ is the exponentially stable equilibrium of the boundary-layer subsystem. This further implies that, for sufficiently large k_2, the sway velocity v_{L} is bounded and furthermore converges to zero very fast, compared to the remaining slow dynamics of $x(t)$, $y(t)$. Then, by substituting the control law (4a) into $\dot{V}$ one gets: $\dot{V} \le -k_1 \left|\boldsymbol{r}_e^\top \left[\begin{smallmatrix}\cos\varphi\\ \sin\varphi\end{smallmatrix}\right]\right| \tanh(\|\boldsymbol{r}_e\|) + \gamma_1(|v_{\mathrm{L}}|)$, where $\gamma_1(\cdot)$ is some class $\mathcal{K}$ function of $|v_{\mathrm{L}}|$, and $\gamma_2(\|\boldsymbol{r}_e\|) = \left|\boldsymbol{r}_e^\top \left[\begin{smallmatrix}\cos\varphi\\ \sin\varphi\end{smallmatrix}\right]\right|$ is also of class $\mathcal{K}$ within the constrained set K_0, due to the geometry of the integral curves of the vector field $\mathbf{F}_{\mathrm{L}}(\cdot)$. Then, V is a local ISS Lyapunov function for the trajectories $\boldsymbol{r}_e(t)$, which further implies that as $v_{\mathrm{L}} \to 0$, then $\boldsymbol{r}_e(t) \to 0$; equivalently, as $v_{\mathrm{L}} \to 0$, the trajectories $\boldsymbol{r}_0(t)$ converge to the desired position $\boldsymbol{r}_{0d}$. ■

In summary, the control law (4) forces L to align with and flow along the vector field $\mathbf{F}_{\mathrm{L}}(\cdot)$. The orientation ψ_{L} is exponentially stable to the reference orientation $\varphi(x_{\mathrm{L}}, y_{\mathrm{L}})$, which by design is equal to $\varphi_p = \operatorname{atan2}(p_y^{\mathrm{L}}, p_x^{\mathrm{L}})$ at the desired position (x_{0d}, y_{0d}). The desired configurations $\boldsymbol{\eta}_{0d}$ such that L lies at a desired distance r_{0d} with T centered in the sensor field-of-view define the manifold $\mathcal{M}_{\mathrm{L}} = \left\{{x_{0d}}^2 + {y_{0d}}^2 = {r_{0d}}^2,\ \psi_d = \operatorname{atan2}(y_{0d}, x_{0d}) + \operatorname{sign}(y_{0d})\pi\right\}$. Thus, any vector $\boldsymbol{p}_{\mathrm{L}}$ such that $\varphi_p = \psi_{\mathrm{L}\,d} \in \mathcal{M}$ creates a reference vector field (3) with integral curves converging to a position $\boldsymbol{r}_{0d} \in \mathcal{M}$. However, not all vector fields defined as above have integral curves such that, if used as reference, guarantee that L will always maintain visibility with T. One option which guarantees visibility maintenance is presented in [18]. Nevertheless, forcing the vehicle to align with the line-of-sight is, on the one hand, not the unique option, while on the other hand, the line-of-sight orientation is not in general an equilibrium point for (1).

3) Switching control for maintaining visibility: Here we propose an alternative control design for ensuring that visibility is always maintained, which is similar to the one in [17]. The idea is that as long as the state trajectories $\boldsymbol{\eta}_0(t)$ evolve away from the boundary ∂K_0, the convergent control law (4) guarantees that the vehicle converges to the desired configuration $\boldsymbol{\eta}_{0d}$; if, on the other hand, the viability of the system is at stake, i.e. if the system trajectories $\boldsymbol{\eta}_0(t)$ reach (close to) the boundary ∂K_0, then switching to a different control law which ensures that the system trajectories will remain into K_0 should occur. Consequently, for redesigning the control law (4) so that the resulting trajectories $\boldsymbol{\eta}_0(t)$ are viable in K_0 we define the continuous switching signals

$$\sigma_{0k}(h_{0k}) = \begin{cases} 0, & h_{0km} < h_{0k} \le 0, \\ \frac{h_{0k} - h_{0kM}}{h_{0km} - h_{0kM}}, & h_{0kM} \le h_{0k} \le h_{0km}, \\ 1, & h_{0k} < h_{0kM}, \end{cases}$$

where $k \in \{1, 2\}$ and h_{0km}, h_{0kM} are a priori defined values for the constraint functions $h_{0k}(\cdot)$, and use the control law:

$$u_{\mathrm{L}} = \sigma_{0k}(h_{0k}) u_{\mathrm{L},conv} + (1 - \sigma_{0k}(h_{0k})) u_{\mathrm{L},viab_k}, \tag{5a}$$

$$r_{\mathrm{L}} = \sigma_{0k}(h_{0k}) r_{\mathrm{L},conv} + (1 - \sigma_{0k}(h_{0k})) r_{\mathrm{L},viab_k}, \tag{5b}$$

where $u_{\mathrm{L},conv}$, $r_{\mathrm{L},conv}$ are the convergent control inputs given by (4), and $u_{\mathrm{L},viab_k}$, $r_{\mathrm{L},viab_k}$ are viable control laws, chosen so that they satisfy the visibility conditions at all points $\bar{\boldsymbol{\eta}}_0$ of the boundary ∂K_0. Consequently, if $h_{0k}(\bar{\boldsymbol{\eta}}_0) = 0$, then one has that $\sigma_{0k}(h_{0k}) = 0$, which ensures that the control law given by (5) at $\bar{\boldsymbol{\eta}}_0 \in \partial K_0$ is viable, i.e. forces the trajectories $\boldsymbol{\eta}_0(t)$ to get back into the interior of K_0, whereas if $\sigma_{0k}(h_{0k}) = 1$, then system viability is not at stake, and the convergent control law (4) applies under (5).

For picking viable control laws $u_{\mathrm{L},viab_1}$, $r_{\mathrm{L},viab_1}$ for the case that the first visibility constraint $h_{01}(\cdot)$ is at stake, one can go with the straightforward option of regulating the orientation ψ_{L} to the angle $\phi_{\mathrm{T}} = \operatorname{atan2}(-y_0, -x_0)$, i.e. to the orientation of the vector $-\boldsymbol{\eta}_0$ connecting L with T; in this way, L is controlled so that T gets centered in the sensor field-of-view. For doing so, one can set the angular velocity controller equal to $r_{\mathrm{L},viab_1} = -k_v(\psi_{\mathrm{L}} - \phi_{\mathrm{T}})$, and keep the linear velocity controller (4a), see also the analysis in [17], [18]. This choice of controllers is sufficient for ensuring that the second constraint $h_{02}(\cdot)$ is never violated as well.

Nevertheless, the control laws $u_{\mathrm{L},viab_k}$, $r_{\mathrm{L},viab_k}$ are not convergent into the ball $\mathcal{B}(\boldsymbol{r}_{0d}, \varepsilon_{\mathrm{L}})$, and therefore the control law (5) does no longer ensure convergence of the position trajectories $\boldsymbol{r}_0(t)$ into $\mathcal{B}(\boldsymbol{r}_{0d}, \varepsilon_{\mathrm{L}})$. In this case, we relax the requirement on the convergence into $\mathcal{B}(\boldsymbol{r}_{0d}, \varepsilon_{\mathrm{L}})$ where $\boldsymbol{r}_{0d}$ a single point, and rather consider the set $C_{\mathrm{L}} \subset K_0$ as: $C_{\mathrm{L}} = \left\{\boldsymbol{\eta}_{0d} \in K_0 \;\middle|\; {x_{0d}}^2 + {y_{0d}}^2 = d^2, \psi_{0d} = \operatorname{atan2}(-y_{0d}, -x_{0d})\right\}$, where $d = \|\boldsymbol{r}_{0d}\|$ is the desired distance w.r.t. the target T. L is then forced to converge to C_{L} under the control law (5), where $u_{\mathrm{L},conv}$, $r_{\mathrm{L},conv}$ are given by (4), while

$$u_{\mathrm{L},viab_k} = -k_1 \operatorname{sgn}\left(\boldsymbol{p}_{\mathrm{L}}^\top \boldsymbol{r}_e\right) \tanh(\|\boldsymbol{r}_e\|), \tag{6a}$$

$$r_{\mathrm{L},viab_k} = -k_v(\psi_{\mathrm{L}} - \psi_d), \tag{6b}$$

where $k_1,\ k_v > 0$, $\boldsymbol{r}_e \triangleq \boldsymbol{r}_0 - \boldsymbol{r}_{0d}$, $\boldsymbol{r}_{0d} = [x_{0d}\ \ y_{0d}]^\top$, $\psi_d = \phi_{\mathrm{T}} = \operatorname{atan2}(-y_0, -x_0)$, $x_{0d} = d\cos\psi_d$, $y_{0d} = d\sin\psi_d$.

B. Control design for the Follower

The control design for F falls in the same spirit; recall that the position $\boldsymbol{r}_1 = [x_1\ \ y_1]^\top$ and the orientation β w.r.t. the leader frame $\mathcal{B}_{\mathrm{L}}$ are measured online, yet F can not access the leader velocities $u_{\mathrm{L}}(t)$, $v_{\mathrm{L}}(t)$, $r_{\mathrm{L}}(t)$ at each time instant t. Nevertheless, L was shown to move with upper bounded velocities, and therefore it is reasonable to assume that F has a priori knowledge on the velocity bounds of L.

The task for F is set as to keep a fixed distance r_{1d} w.r.t. L with angle $\phi_1 = 0$, so that L is centered in the camera field-of-view (f.o.v.). This requirement specifies a manifold $\mathcal{M}_{\mathrm{F}} = \left\{{x_{1d}}^2 + {y_{1d}}^2 = {r_{1d}}^2, \psi_{\mathrm{F}\,d} = \operatorname{atan2}(y_{1d}, x_{1d}) + \operatorname{sign}(y_{1d})\pi\right\}$ of desired configurations for F.

Therefore, the control objective for F reads as to converge and remain into a ball $\mathcal{B}(\boldsymbol{r}_{1d}, \varepsilon_{\mathrm{F}})$ of radius $\varepsilon_{\mathrm{F}} > 0$ around a desired position $\boldsymbol{r}_{1d} \in \mathcal{M}_{\mathrm{F}}$.

Theorem 2: The trajectories $\boldsymbol{r}_1(t) = [x_1(t) \;\; y_1(t)]^\top$ of F enter and remain into a ball $\mathcal{B}(\boldsymbol{r}_{1d}, \varepsilon_\text{F})$ around the desired position $\boldsymbol{r}_{1d}$, under the (virtual) control law

$$u_\text{F} = -k_3 \,\text{sgn}(\boldsymbol{p}_\text{F}^\top \boldsymbol{r}_e) \tanh(\|\boldsymbol{r}_e\|) - \text{sgn}(\boldsymbol{p}_\text{F}^\top \boldsymbol{r}_e)|k_1|, \quad (7a)$$
$$r_\text{F} = -k_4(\beta - \varphi) + \dot{\varphi}, \quad (7b)$$

where $k_3,\ k_4 > 0$, $\boldsymbol{r}_e = \boldsymbol{r}_1 - \boldsymbol{r}_{1d}$, φ is the orientation of the vector field $\mathbf{F}_\text{F}(\cdot)$ at (x_1, y_1), k_1 is the upper bound of the linear velocity of L. The proof follows the standard practice also used in [18] and is omitted here for the interest of space. Finally, the dynamic control inputs are defined as:

$$\tau_{ui} = m_u \alpha_i - m_v v r - X_u u - X_{u|u|}|u|u + |w_u|, \quad (8a)$$
$$\tau_{ri} = m_r \beta_i - m_{uv} u r - N_r r - N_{r|r|}|r|r + |w_r|, \quad (8b)$$
$$\alpha_i = -k_u(u - \gamma_{i1}(\cdot)) + \tfrac{\partial \gamma_1}{\partial \boldsymbol{\eta}_i} \dot{\boldsymbol{\eta}}_i, \quad k_u > 0, \quad (8c)$$
$$\beta_i = -k_r(r - \gamma_{i2}(\cdot)) + \tfrac{\partial \gamma_2}{\partial \boldsymbol{\eta}_i} \dot{\boldsymbol{\eta}}_i, \quad k_r > 0. \quad (8d)$$

where $\gamma_{i1}(\cdot)$, $\gamma_{i2}(\cdot)$ are the virtual linear and angular velocity, respectively, for each vehicle i, given by (5), (7). It is easy to verify that the tracking errors $u_i - \gamma_{i1}(\cdot)$, $r_i - \gamma_{i2}(\cdot)$ are ISS and asymptotically converge to $|w_u|$, $|w_r|$, respectively. The proof is omitted for the interest of space.

IV. Simulation Results

The efficacy of the proposed control algorithm is demonstrated through computer simulations. The vehicles initiate at $\boldsymbol{\eta}_\text{L}(0) = [-0.9 \;\; 0.4 \;\; 0]^\top$ and $\boldsymbol{\eta}_\text{F}(0) = \left[-0.9 \;\; 0 \;\; \frac{\pi}{2}\right]^\top$, so that the target T, positioned at $(0.3, 0)$ is visible to L.

For demonstrating the robustness of the algorithms against bounded, non-vanishing disturbances, we consider two cases, see Fig. 2 and Fig. 3. The model parameters have been taken out of [22]. As expected, L moves to maintain a desired distance and visibility w.r.t. T (Fig. 4(a), 5(a)), and F maintains visibility and keeps a fixed distance w.r.t. L, while also avoiding inter-vehicle collisions (Fig. 4(a), 4(b), 5(b), 5(c)). The control design for L allows the orientation ψ_L to take values that are closer to the boundary $h_{01}(\cdot) = 0$, compared to the orientation control design for F, which aligns the vehicle along the line-of-sight w.r.t. L. For the interest of space we have not plotted the evolution of the constraint functions $h_{j2}(\cdot) = \|\boldsymbol{r}_j\| - L \leq 0$, where $L = 1.2$ m; nevertheless it is easy to verify out of Fig. 4(b), 5(c) that the values of $h_{j2}(\cdot)$ always remain negative as well.

V. Conclusions

This paper presented a L − F formation control strategy for underactuated marine vehicles with sensing and communication limitations, which can be used for surveillance of stationary targets in the presence of bounded, persistent environmental disturbances. A cooperative formation control scheme was developed based on concepts from viability theory and on the notion of dipolar vector fields. The efficacy of the proposed algorithm was demonstrated through computer simulations. Future work can be towards extending the methodology in the case of multiple moving targets (evaders) and multiple vehicles (pursuers).

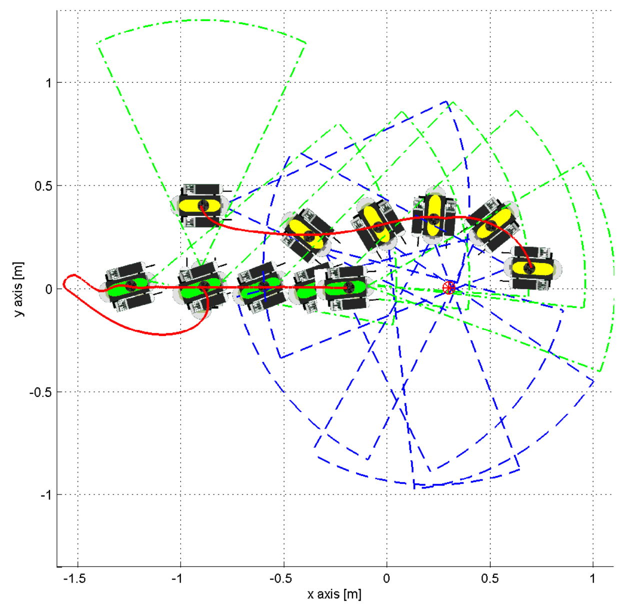

Fig. 2. The paths followed by the marine vehicles in the case of non-vanishing, bounded external disturbances $\boldsymbol{w}$.

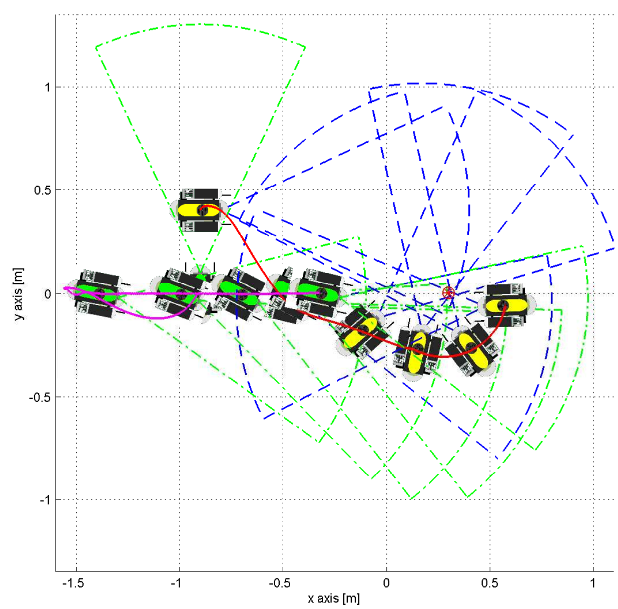

Fig. 3. The paths followed by the marine vehicles in the case of non-vanishing, bounded external disturbances $-\boldsymbol{w}$.

References

[1] E. Børhaug, A. Pavlov, R. Ghabcheloo, K. Y. Pettersen, A. Pascoal, and C. Silvestre, "Formation control of underactuated marine vehicles with communication constraints," in *Proc. of the 7th IFAC Conference on Manoeuvring and Control of Marine Craft*, Lisbon, Portugal, 2006.

[2] R. Ghabchello, A. P. Aguiar, A. Pascoal, C. Silvestre, I. Kaminer, and J. Hespanha, "Coordinated path-following in the presence of communication losses and time delays," *SIAM Journal on Control and Optimization*, vol. 48, no. 1, pp. 234–265, 2009.

[3] M. Burger, A. Pavlov, E. Børhaug, and K. Pettersen, "Straight line path following for formations of underactuated surface vessels under influence of constant ocean currents," in *Proc. of the 2009 American Control Conference*, St. Louis, MO, USA, Jun. 2009, pp. 3065–3070.

[4] Y. Wang, W. Yan, and J. Li, "Passivity-based formation control of autonomous underwater vehicles," *IET Control Theory and Applications*, vol. 6, no. 4, pp. 518–525, 2012.

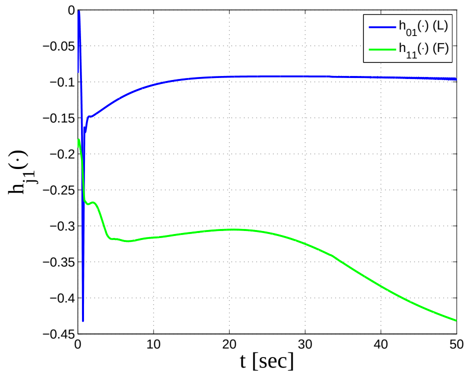

(a) The visibility constraints $h_{j1}(\cdot) \leq 0$, $\forall t$, for L, F

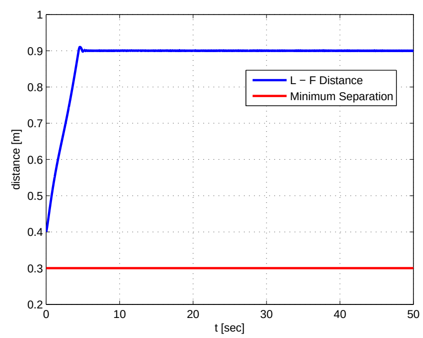

(b) F converges to and maintains fixed distance w.r.t. L.

Fig. 4. Constraint evolution against persistent bounded disturbances $\boldsymbol{w}$.

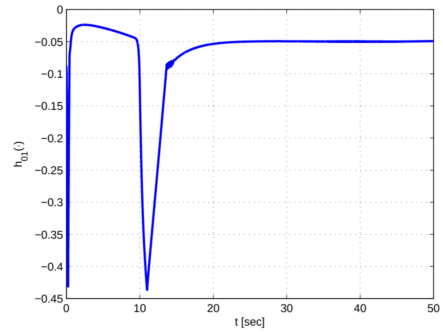

(a) The visibility constraint $h_{01}(\cdot) \leq 0$, $\forall t$, for L.

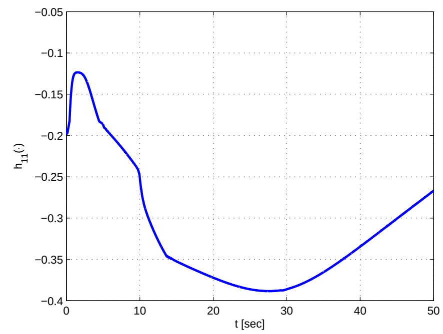

(b) The visibility constraint $h_{11}(\cdot) \leq 0$, $\forall t$, for F.

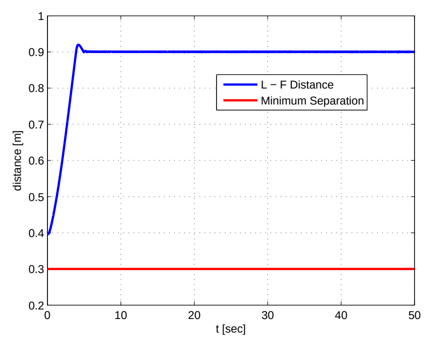

(c) F converges to and maintains fixed distance w.r.t. L.

Fig. 5. Constraint evolution against persistent bounded disturbances $-\boldsymbol{w}$.

[5] M. Burger and K. Pettersen, “Curved trajectory tracking for surface vessel formations,” in *Proc. of the 49th IEEE Conference on Decision and Control*, Atlanta, GA, USA, Dec. 2010, pp. 7159–7165.

[6] Z. Peng, D. Wang, W. Lan, X. Li, and G. Sun, “Decentralized cooperative control of autonomous surface vehicles with uncertain dynamics: A dynamic surface approach,” in *Proc. of the 2011 American Control Conference*, San Francisco, CA, USA, Jun. 2011, pp. 2174–2179.

[7] F. Arrichiello, S. Chiaverini, and T. I. Fossen, “Formation control of underactuated surface vessels using the null-space-based behavioral control,” in *Proc. of the 2006 IEEE/RSJ Int. Conf. on Intelligent Robots and Systems*, Beijing, China, Oct. 2006, pp. 5942–5947.

[8] F. Arrichiello, J. Das, H. Heidarsson, A. Pereira, S. Chiaverini, and G. Sukhatme, “Multi-robot collaboration with range-limited communication: Experiments with two underactuated ASVs,” in *Proc. of the 2009 International Conference on Field and Service Robotics*, Cambridge, MA, USA, Jul. 2009.

[9] I.-A. F. Ihle, J. Jouffroy, and T. I. Fossen, “Formation control of marine surface craft: A Lagrangian approach,” *IEEE Journal of Oceanic Engineering*, vol. 31, no. 4, pp. 922–934, Oct. 2006.

[10] H. Yang and F. Zhang, “Geometric formation control for autonomous underwater vehicles,” in *Proc. of the 2010 IEEE Int. Conf. on Robotics and Automation*, Anchorage, Alaska, May 2010, pp. 4288–4293.

[11] D. B. Eduards, T. A. Bean, D. L. Odell, and M. J. Anderson, “A leader-follower algorithm for multiple AUV formations,” in *Proc. of the 2004 IEEE/OES Autonomous Underwater Vehicles*, Jun. 2004, pp. 40–46.

[12] S. Emrani, A. Dirafzoon, and H. A. Talebi, “Leader-follower formation control of autonomous underwater vehicles with limited communications,” in *Proc. of the 2011 IEEE Int. Conf. on Control Applications (CCA)*, Denver, CO, USA, Sep. 2011, pp. 921–926.

[13] T. Ikeda, T. Mita, and M. Yamakita, “Formation control of autonomous underwater vehicles,” in *16th IFAC World Congress*, Prague, Czech Republic, Jul. 2005.

[14] F. Fahimi, “Sliding mode formation control for under-actuated autonomous surface vehicles,” in *Proc. of the 2006 American Control Conference*, Minneapolis, Minnesota, USA, Jun. 2006, pp. 4255–4260.

[15] R. Cui, S. S. Ge, B. V. E. How, and Y. S. Choo, “Leader-follower formation control of underactuated autonomous underwater vehicles,” *Ocean Engineering*, vol. 37, pp. 1491–1502, 2010.

[16] X. Xiang, B. Jouvencel, and O. Parodi, “Coordinated formation control of multiple autonomous underwater vehicles for pipeline inspection,” *International Journal of Advanced Robotic Systems*, vol. 7, no. 1, pp. 75–84, 2010.

[17] D. Panagou and K. J. Kyriakopoulos, “Control of underactuated systems with viability constraints,” in *Proc. of the 50th IEEE Conference on Decision and Control and European Control Conference*, Orlando, Florida, Dec. 2011, pp. 5497–5502.

[18] D. Panagou and V. Kumar, “Maintaining visibility for leader-follower formations in obstacle environments,” in *Proc. of the 2012 IEEE Int. Conf. on Robotics and Automation*, St. Paul, Minnesota, USA, May 2012, pp. 1811–1816.

[19] J.-P. Aubin, *Viability Theory*. Birkhäuser, 1991.

[20] T. I. Fossen, *Marine Control Systems: Guidance, Navigation and Control of Ships, Rigs and Underwater Vehicles*. Marine Cybernetics.

[21] H. K. Khalil, *Nonlinear Systems. Third Edition*. Prentice-Hall, 2002.

[22] W. Wang and C. M. Clark, “Modeling and simulation of the videoray pro iii underwater vehicle,” in *Proc. of OCEANS 2006 - Asia Pacific*, Singapore, May 2006, pp. 1–7.